ELSEVIER

Journal of Molecular Catalysis A: Chemical 162 (2000) 335–352

JOURNAL OF MOLECULAR CATALYSIS A: CHEMICAL

www.elsevier.com/locate/molcata

Adsorption and reactions of CH_3Cl on Mo_2C based catalyst

J. Cserényi *, L. Óvári, T. Bánsági, F. Solymosi

Institute of Solid State and Radiochemistry, University of Szeged and Reaction Kinetics Research Group of the Hungarian Academy of Sciences[1], P.O. Box 168, H-6701, Szeged, Hungary

Abstract

The adsorption of CH_3Cl on ZSM-5, Mo_2C/ZSM-5 and Mo_2C/SiO_2 was investigated by temperature-programmed desorption (TPD) and Fourier transform infrared spectroscopy (FTIR). The formation of methoxy species was clearly identified on all the three catalysts. Three elementary steps were considered to explain the absorption bands observed in the IR spectra and to describe the reaction products found at higher temperatures: (i) the interaction of CH_3Cl with the OH groups of ZSM-5, (ii) dissociation of CH_3Cl yielding CH_3, and (iii) the elimination of HCl from the adsorbed CH_3Cl to give CH_2 species. A new finding was the identification of the alkenyl carbocation formed on the Lewis acidic sites of ZSM-5. The decomposition of CH_3Cl on ZSM-5 proceeded at 673 K with a high conversion yielding propylene, ethylene, butane, methane and benzene in decreasing selectivities. Deposition of Mo_2C on ZSM only slightly modified the catalytic behavior of ZSM-5. Its promoter effect came into prominence on silica surface.

Keywords: Adsorption and reactions; CH_3Cl; Mo_2C-based catalyst

1. Introduction

The catalytic conversion of methane into more valuable compounds has been the subject of intensive research during the last two decades. One of the ways is to convert methane to methyl chloride via oxychlorination reaction [1,2], and then transform methyl chloride into light olefins and hydrochloric acid [3,4]. Pure and modified ZSM-5 is an effective catalyst for CH_3C1 reaction, the product distribution sensitively depends on the reaction temperature and on the nature of the promoters [5–8].

Recently, it was found that Mo_2C deposited on the cavities of ZSM-5 is an active catalyst in the direct conversion of methane into benzene [9–12]. The same results were observed when the starting material was MoO_3/ZSM-5 [13–15], as MoO_3 was converted into Mo_2C during the high temperature reaction [9–12]. It was thought that the primary role of Mo_2C is to activate methane to produce CH_3 and/or CH_2 species and then — through their coupling — ethane and/or ethylene. The oligomerization and aromatization of these compounds proceed on the ZSM-5. In the subsequent studies, it was found that Mo_2C also exerts a promoting influence even on the aromatization of ethane and propane, which occurs readily on ZSM-5 [16,17].

In the present work, an attempt is being made to examine the effect of Mo_2C on the interaction and

* Corresponding author.

[1] These laboratories are parts of the Center for Catalysis, Surface and Material Science at the University of Szeged.

1381-1169/00/$ - see front matter
PII: S1381-1169(00)00301-0

reaction of CH_3C1 with ZSM-5. It is hoped that the results obtained may also contribute to the better understanding of the aromatization of methane on this catalyst.

2. Experimental

Catalytic reactions were carried out at 1 atm of CH_3Cl + Ar gas mixture containing 5% of CH_3Cl in a fixed-bed, continuous flow reactor consisting of a quartz tube (10 mm i.d.) connected to a capillary tube. The flow rate was 12 ml/min. Generally, 0.5 g of loosely compressed catalyst sample was used. Reaction products were analyzed by means of a Hewlett-Packard 5890 gas chromatograph using a Porapak QS column. The conversion of CH_3Cl was calculated from the hydrogen balance. The selectivity values of product formation represent the fraction of methyl chloride that has been converted into specific products, taking into account the number of carbon atoms in the molecules. The decomposition of CH_3Cl was also followed in a closed circulation system, where the analysis of products was performed by a mass spectrometer.

Infrared spectroscopic measurements were made in a vacuum IR cell using self-supporting wafers of catalyst powders. Spectra were recorded with a Biorad (Digilab. Div.) Fourier transform IR spectrometer FTS 155.

The H-ZSM-5 support was obtained by five times repeated ion exchange of Na-ZSM-5 (Si/Al = 55.0) with an aqueous solution of ammonium nitrate (1N), and calcined in air at 863 K for 5 h. Before catalytic measurements, each sample was oxidized in an O_2 stream at 973 K in situ and then flushed with Ar for 15 min. Hexagonal Mo_2C was prepared by the method of Lee et al. [18]. Briefly, about 0.5 g of MoO_3 was heated in 1:4 methane–H_2 mixture flowing at 300 ml (STP)/min in a quartz cell with two stopcocks. Preparation temperature was increased rapidly to 773 K and at 30 K/h between 773 and 1023 K, and maintained at 1023 K for 3 h.

Supported Mo_2C was produced by the carburation of supported MoO_3 in the catalytic reactor, in a similar way as described above for the preparation of bulk Mo_2C. MoO_3/ZSM-5 and MoO_3/SiO_2 were prepared by impregnating the supports with a basic solution of ammonium paramolybdate to yield a nominal 2 wt.% of MoO_3. The suspension was dried at 373 K and calcined at 873 K for 5 h. Following the suggestion of Lee et al. [18], the sample was deactivated at 300 K with air, or used in situ for catalytic studies. As Mo_2C always contains excess carbon, the catalyst was treated with H_2 at 873 K before the catalytic measurements to remove this carbon species. The gases used were of commercial purity (Linde). Ar (99.996%) and H_2 (99.999%) were deoxygenated with an oxytrap. The other impurities were adsorbed by a 5A molecular sieve at the temperature of liquid nitrogen.

3. Results

3.1. Adsorption of CH_3Cl

3.1.1. Temperature-programmed desorption (TPD) measurements

The interaction of CH_3Cl with the above catalysts has been first studied by means of TPD. A 0.5-g catalyst sample was kept in CH_3Cl flow at 373 K for 10 min, afterwards, the reactor was washed with argon until no or only traces of CH_3Cl was detected in the outlet gas; this required about 60 min. TPD spectra are shown in Fig. 1. CH_3Cl desorbed from the ZSM-5 with a peak temperature $T_p = 393$ K. Methane and hydrogen were released only above 700 K. Similar features have been observed for the Mo_2C/ZSM-5 sample. The amount of CH_3Cl desorbed was somewhat less, but the peak temperature was the same. At the same time, however, the formation of methane ($T_p = 420$ K), ethylene ($T_p = 550$ K) and propane was observed.

3.1.2. Infrared spectroscopic measurements

The ZSM-5 sample exhibited the usual absorption bands at 3744, 3679 and 3612 cm^{-1}. These bands are assigned to terminal Si–OH groups, Al–OH groups and acidic bridging hydroxyls, respectively. The deposition of Mo_2C onto ZSM-5 did not alter this picture, except that the intensity of the 3612 cm^{-1} band has been reduced by about 40%.

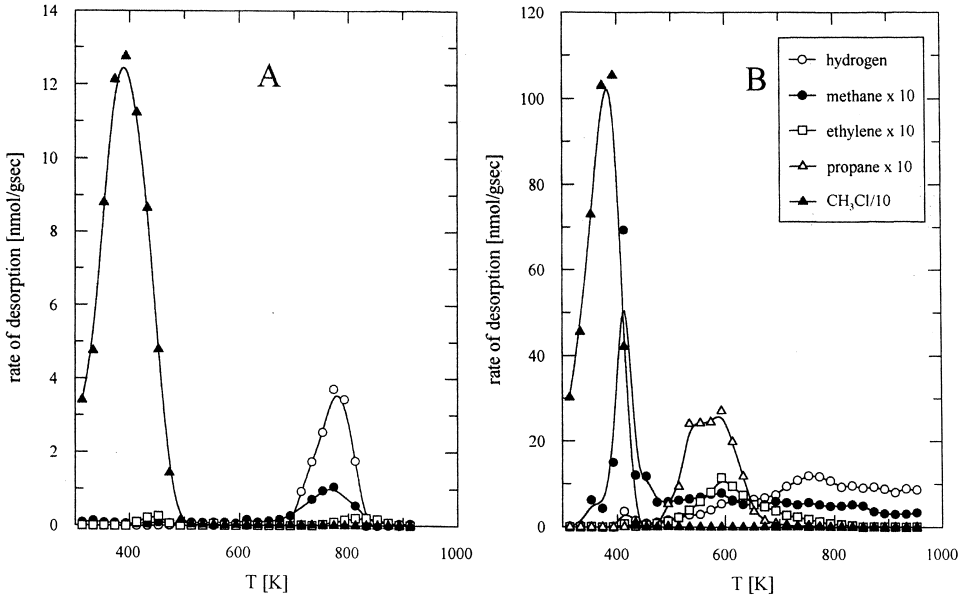

Fig. 1. TPD spectra following the adsorption of CH_3Cl on (A) ZSM-5 and (B) Mo_2C/ZSM-5 samples at 373 K.

Fourier transform infrared spectroscopy (FTIR) spectra of adsorbed CH_3Cl on Mo_2C/ZSM-5 are shown in Fig. 2. Absorption bands observed at 2963, 2860, 1444 and 1350 cm^{-1} correspond well to different vibrations of adsorbed CH_3Cl. The assignment of these bands is presented in Table 1. In the OH frequency region, reverse absorption bands developed at 3663 and 3612 cm^{-1}, and a broad band at 3175 cm^{-1}. Degassing the sample at room temperature resulted in the elimination of all bands, including the reverse absorption bands, indicating the weak interaction at 300 K. When the sample was kept in 10 Torr of CH_3Cl at 473 K and evacuated at 300 K, both reverse bands at 3663 and 3612 cm^{-1} remained

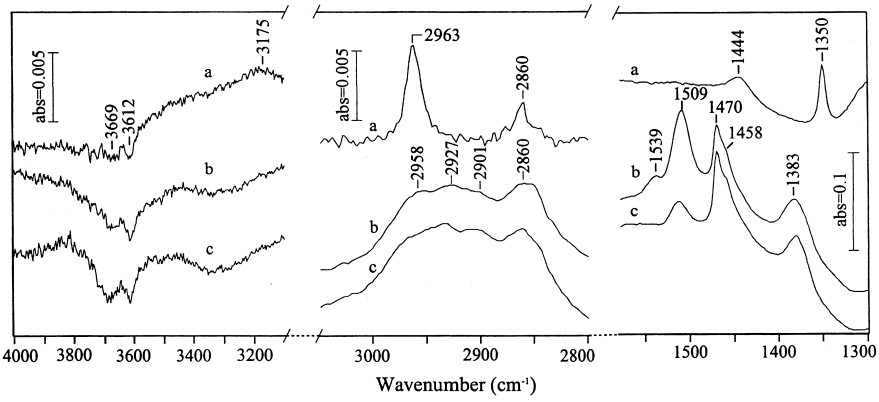

Fig. 2. (a) FTIR spectra of Mo_2C/ZSM-5 in the presence of CH_3Cl (10 Torr) at 300 K (the spectrum of gas phase is subtracted), and after adsorption of CH_3Cl at 473 (b) and 573 K (c). In the latter two cases, the sample was degassed at 300 K.

Table 1
Characteristic vibrations of different adsorbed species

Assignments	CH_3Cl gas [22]	CH_3Cl Mo_2C/ ZSM-5 300 K[a]	CH_3Cl Mo_2C/ ZSM-5 473 K[a]	CH_3Cl Mo_2C/ SiO_2 473 K[a]	CH_3 Mo_2C [20]	CH_2 Mo_2C [19]	C_2H_4 ZSM-5 153 K[a]	di-σ C_2H_4 (4×4)-C/ Mo(110) [23]	CCH_3 (4×4)-C/ Mo(110) [23]	di-σ propylene Pt/SiO_2 [24]	CH_3O SiO_2 [27]	C_2H_5O SiO_2 [26]	C_3H_7O TiO_2 [25]
$\nu_{as}(CH_3)$	3042	–	2958 (w)	2961 (m)	2930 (m)						3001 (w), 2961 (m)	2986 (s)	2965 (s)
$\nu_{as}(CH_2)$			2927 (w)			2940 (s)	3090	3010 (w)				2940 (m)	2940 (m)
$\nu_s(CH_3)$	2966	2963 (w)	2901 (vw)	2859 (m)					2915 (s)	2885 (m)	2859 (m)	2911 (m)	2885 (s)
$\nu_s(CH_2)$			2860 (w)				2975	2935(s)		2920 (ms)		2882 (w)	2855 (w)
$2\delta_{as}(CH_3)$	2879	2860 (w)		2939 (w)							2937 (w)		
ν(C=C)			1539 (m)				1631, 1612						
ν_{as}(CCC)			1509 (vs)										
$\delta_{as}(CH_3)$	1455	1444 (m)	1458 (m)	1464 (w)	1370 (m)				1430 (m)	1465 (w)	1481 (w)	1452 (w)	
$\delta(CH_2)$			1470 (vs)				1441,1340	1395 (s)				1492 (w)	1460 (m)
$\delta_s(CH_3)$	1355	1350 (s)	1383 (s)	1441 (w)	1180 (s)	780			1345 (m)	1350 (ms)	1466 (s)	1399(m)	1380 (m)
$\rho(CH_2)$												1384 (m)	
$\omega(CH_2)$						1190 (m)		1180 (w)				1348 (m)	
ν(C−C)									1075 (m)				
$\gamma(CH_2)$								1035 (s)					

[a]This work.

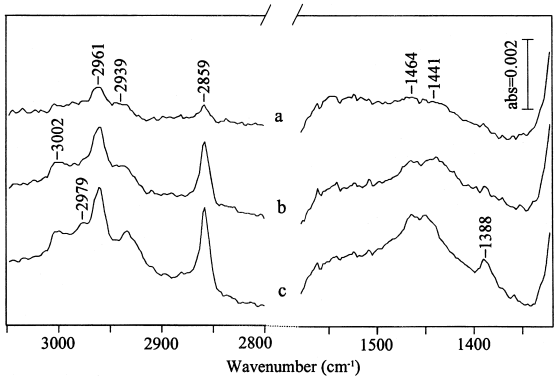

Fig. 3. FTIR spectra of Mo_2C/SiO_2 following the adsorption of CH_3Cl at different temperatures. (a) 473; (b) 573 K; (c) 673 K and degassing at 300 K.

practically unchanged, which is in contrast with the room temperature adsorption. In addition, relatively intense absorption bands developed at 2958, 2927, 2901 and 2860 cm^{-1} in the CH stretching region, and at 1539, 1509, 1470, 1458 and 1383 cm^{-1} in the CH deformation mode. This suggests an activated adsorption of CH_3Cl. Further heating the sample in CH_3Cl to 573 and then to 673 K caused only a slight attenuation of the bands observed after degassing at room temperature. A noteworthy difference was the elimination of the band at 1539 cm^{-1}.

Similar measurements were performed with pure ZSM-5. IR spectra obtained in the presence of CH_3Cl at room temperature exhibited practically the same spectral features as measured for $Mo_2C/ZSM\text{-}5$. No change in the nature of the weak interaction was experienced at 300 K. Treating the sample with 10 Torr of CH_3Cl at different temperatures caused the appearance of the same bands as observed for $Mo_2C/ZSM\text{-}5$.

The adsorption of CH_3Cl on Mo_2C/SiO_2 produced much weaker bands than on the previous samples, and yielded no observable change in the intense OH band of silica at 3746 cm^{-1}. To produce absorption bands surviving room temperature adsorption, we had to keep the sample again in the presence of gaseous CH_3Cl at and above 473 K. In this case, bands were registered at 2961, 2939, 2859, 1446 and 1441 cm^{-1}. The spectra are shown in Fig. 3. We observed a slight enhancement of these bands with the increase of the adsorption temperature, without changing their positions. New bands appeared at 2979 and 1388 cm^{-1} after treating the Mo_2C/SiO_2 sample with CH_3Cl at 673 K. The peaks observed at 473 K for Mo_2C/SiO_2 also appeared on the IR spectrum of pure silica, but with much less intensities. The difference is that the 2939 and 1446 cm^{-1} bands are missing, and the bands at 2979 and 1388 cm^{-1} did not develop at 673 K.

3.2. Catalytic decomposition of CH_3Cl

3.2.1. Measurements in closed system

The reaction of CH_3Cl was first studied in a closed circulation system using a mass spectrometric analysis. A well measurable decomposition of CH_3Cl on Mo_2C/SiO_2 occurred above 650 K. The main

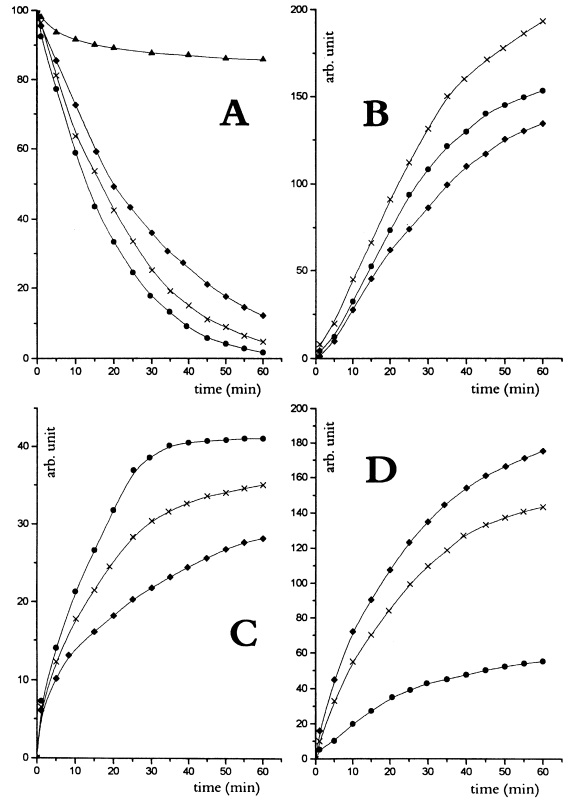

Fig. 4. Decomposition of CH_3Cl on $Mo_2C/ZSM\text{-}5$ (x), Mo_2C/SiO_2 (♦) ZSM-5 (●) and SiO_2 (▲) at 743 K followed by mass spectrometric analysis. Conversion of CH_3Cl (A), formation of HCl (B), C_2H_4 (C) and CH_4 (D).

products were CH_4, C_2H_4 and HCl. At 743 K, the CH_4/C_2H_4 ratio is in the range of 4.5–4.9. Note that silica support is practically inactive towards the decomposition of CH_3Cl. On the other hand, ZSM-5 alone is quite an effective catalyst yielding the same products: the CH_4/C_2H_4 ratio varied between 1.0–1.2. The deposition of Mo_2C on ZSM-5 in highly dispersed state caused only little promoting effect both for the conversion and product distribution. The CH_4/C_2H_4 ratio was about 3.2. The conversion of CH_3Cl and the formation of products on different samples are displayed in Fig. 4.

3.2.2. Flow system

More detailed measurements have been carried out in a flow system. At 673 K, the extent of the decomposition attained a value of 92–93% for ZSM-5 and 72–73% for Mo_2C/ZSM-5. Both samples exhibited constant activity. The products in decreasing selectivities are propylene, butane, ethylene, methane and benzene. Ethane and propane were detected only in trace amounts. Results are collected in Table 2. The differences between the two samples are that more methane and benzene formed on the Mo_2C-containing ZSM-5. The effect of Mo_2C was more pronounced when it was deposited on silica, which was practically inactive at 673 K. In this case, the initial conversion was 4.2%, which slowly decreased to 1.2%. The product distribution basically differed from that observed for the previous samples: the selectivity to methane was 77% followed by ethylene (18%) and propylene (4%). Note that the decomposition of CH_3Cl on pure Mo_2C in a flow system amounts only to 0.03–0.04% at 673 K.

Table 2
Conversion of CH_3Cl and selectivities for various products on different catalyst at 673 K

	ZSM-5	Mo_2C/ ZSM-5	Mo_2C/ SiO_2
Conversion %			
	92.5	72.5	4.2
Selectivities %			
CH_4	1.0	5.0	77.0
C_2H_4	16.0	17.0	18.0
C_2H_6	–	–	–
C_3H_6	54.0	53.0	4.0
C_3H_8	–	–	–
C_4'S	26.0	17.0	–
C_6H_6	0.5	5.0	–

4. Discussion

4.1. Reactivities of C_xH_y fragments on Mo_2C

For the interpretation of the results obtained, it is helpful to summarize the main characteristics of different hydrocarbon fragments on Mo_2C surface. Recently, we examined the adsorption and dissociation of CH_2I_2, CH_3I and C_2H_5I on Mo_2C and the reaction pathways of the hydrocarbons formed [19,20]. Whereas CH_2 and CH_3 underwent fast decomposition on Pt metals producing only minor quantities of C_2 compounds [21] on Mo_2C, the tendency of the coupling of CH_2 and CH_3 was much greater than on these metals. Surprisingly, the formation of C_2H_4 also occurred in the reaction of CH_3 on Mo_2C, which was not detected at all for Pt metals [21]. In contrast with this, the reaction of C_2H_5 did not differ much on Pt metals and Mo_2C [20]: the C–C bond remained intact on both types of solids.

4.2. TPD and IR spectroscopic studies

TPD measurements showed that following the adsorption of CH_3Cl on ZSM-5 at 373 K, a fraction of it remained adsorbed and was released with a $T_p = 393$ K. The presence of Mo_2C did not influence this peak temperature, suggesting that most of the CH_3Cl adsorbed on the ZSM-5. That fact that the desorbing amount of CH_3Cl somewhat decayed shows that Mo_2C blocks some of the adsorption sites on the ZSM-5. In addition, the formation of other products was clearly enhanced by the presence of Mo_2C. This feature indicates that Mo_2C can induce the dissociation of CH_3Cl at such a low temperature, where ZSM-5 alone is not effective.

IR spectroscopic measurements suggest that CH_3Cl adsorbs molecularly on all the three samples, ZSM-5, Mo_2C/ZSM-5 and Mo_2C/SiO_2 at 300 K. Absorption bands detected are readily assigned to the vibrations of adsorbed CH_3Cl [22] (Table 1). All

these bands were eliminated after evacuation at room temperature indicating the weakness of the adsorption. At and above 473 K, however, the nature of the adsorption basically altered. This was first exhibited by the development of reverse bands at 3669 and 3612 cm^{-1} in the OH frequency region for $Mo_2C/ZSM\text{-}5$ and ZSM-5, and the appearance of stable absorption bands at 2958, 2927, 2901, 2860, 1539, 1509, 1470, 1458 and 1383 cm^{-1} (Fig. 2). In order to facilitate the interpretation of these spectral features, the characteristic bands of all compounds possibly formed are collected in Table 1. As spectra measured after the adsorption of CH_3Cl on ZSM-5 and $Mo_2C/ZSM\text{-}5$ at 473 K and subsequent evacuation at room temperature were almost identical, we can say that surface species originating these bands are bonded to the zeolite surface. It is important to point out that the intense band of CH_3Cl at 1350 cm^{-1} is missing from the spectra taken at elevated temperatures, suggesting that intact CH_3Cl did not remain on the surface. The reverse bands at 3669 and 3612 cm^{-1} unambiguously show the occurrence of a surface process between the OH groups of the zeolite and adsorbed CH_3Cl

$$CH_3Cl_{(a)} + OH_{(a)} = CH_3O_{(a)} + HCl_{(g)} \quad (1)$$

Similar spectral changes were found for acidic zeolite, HY-FAU, but were not observed for basic sample, Na/NaY-FAU [28]. The formation of methoxy species has been identified by IR spectroscopy following the adsorption of CH_3Cl on a number of oxides [29,30]. Its production was also established on Pd/SiO_2 after the activation of CH_3Cl by palladium [31], and in the direct interaction of CH_3 stream with Rh/SiO_2, SiO_2 and TiO_2 [32,33]. Accepting this consideration, the bands at 2958 and 2860 cm^{-1} can be attributed to the $\nu_{as}(CH_3)$ and $\nu_s(CH_3)$ modes, whereas the bands at 1470 and 1458 cm^{-1} to the $\delta_{as}(CH_3)$ and $\delta_s(CH_3)$ in CH_3O. The more characteristic band at 1060 cm^{-1} due to the vibration of $\nu(CO)$ in methoxy is missing, but the detection of this band on zeolite and silica is extremely difficult.

In addition to the above process, we can also consider two other elementary reactions, the elimination of HCl

$$CH_3Cl_{(a)} = CH_{2(a)} + HCl_{(a)} \quad (2)$$

and the cleavage of Cl–C bond

$$CH_3Cl_{(a)} = CH_{3(a)} + Cl_{(a)} \quad (3)$$

The formation of both the CH_3 and the CH_2 species was observed in the dissociation of the corresponding iodo compounds on $Mo_2C/Mo(100)$ surface in UHV system [19,20]. They existed on the surface up to 250–300 K. IR spectra presented in Fig. 2 also suggest that they have been converted into other surface species after their formation, which is consistent with their high reactivity.

Accordingly, we can count with the coexistence of two or more adsorbed species on the surface at and above 473 K. The primary products of the coupling of CH_3 and CH_2 are ethane and ethylene. From these two compounds, ethylene forms a stable adsorbed species on the catalyst surface. However, on $Mo_2C/Mo(100)$, even the more stable di-σ-bonded ethylene has been transformed into ethylidyne in the temperature range of 260–350 K [23]. The absence of absorption bands at 1430 and 1345 cm^{-1} due to $\delta_{as}(CH_3)$ and $\delta_{sym}(CH_3)$ of ethylidyne excludes its formation in the present case. Note that neither di-σ-bonded ethylene nor ethylidyne exists on ZSM-5. We can also consider the formation of adsorbed ethoxy, which could be a surface intermediate in the production of ethylene from CH_3Cl [8], as described in Scheme 1.

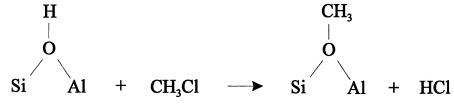

(4)

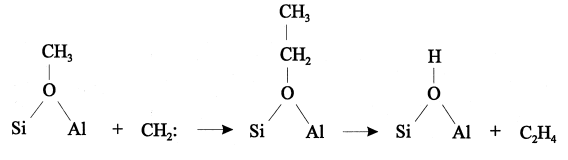

(5)

As we identified propylene in the products of the catalytic transformation of CH_3Cl, we propose the

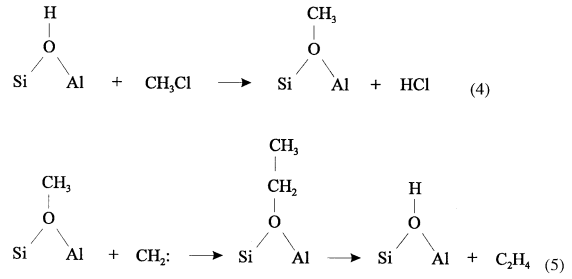

Scheme 1.

insertion of a second carbene to ethoxy to give adsorbed propoxide, the decomposition of which yields propylene

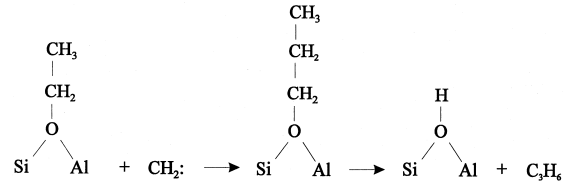

(6)

On the basis of broad absorption in the frequency range between 2800 and 3000 cm^{-1} (Fig. 2), as well as on that of the vibration data of Table 2, we cannot exclude the contribution of vibrations of ethoxy and propoxy surface complexes to the observed absorption bands.

However, neither of the adsorbed species assumed so far explains the origin of the intense band at 1509 cm^{-1}, which was detectable up to 573 K. This band has been identified following the adsorption of methanol and alkenes on protonic zeolites in a number of cases [34], and was attributed to the ν_{as}(C–C–C) stretching mode of alkenyl carbocations having an extremely high extinction coefficient [34]. In the present case, its formation could occur in the strong interaction of propylene with the Lewis acidic sites (L) of ZSM-5

$$C_3H_{6(a)} + L \rightarrow L - H^- + C_3H^+_{5(a)} \quad (7)$$

Control measurements confirmed this assumption, as exposing ZSM-5 to propylene at and above 473 K, a strong absorption band developed at 1509 cm^{-1}, which was eliminated only at 623 K.

The adsorption of CH_3Cl on Mo_2C/SiO_2 is also molecular and reversible at 300 K. A stronger interaction was measured only at and above 473 K, when absorption bands at 2961, 2939, 2859, 1464 and 1441 cm^{-1} remained on the spectrum after room temperature evacuation. These bands can be attributed to the different vibrations of methoxy species (Table 2). On pure SiO_2, the intensities of absorption bands, particularly in the low frequency regions, were much weaker, and the band at 1441 cm^{-1} was even missing. This suggests that the formation of methoxy on silica is promoted by Mo_2C. It is very likely that CH_3Cl dissociates on Mo_2C (Eq. 3), and the CH_3 formed migrates onto silica to give CH_3O. This way of methoxy formation was proposed first in the case of Pd/SiO_2 [31].

It is important to emphasize that we could not detect an absorption band at 1509 cm^{-1} for this sample under any experimental conditions. This is consistent with the consideration presented for the assignment of this band. For the formation of carbocations, the presence of surface acid centers is a prerequisite. Due to lack of this center on Mo_2C/SiO_2, carbocations cannot be produced.

4.3. Catalytic decomposition

Studies performed in closed circulation system clearly showed that Mo_2C deposited onto SiO_2 catalyzes the decomposition of CH_3Cl. This was confirmed by the results obtained in a flow system, where the main products of the reaction were methane and ethylene, with a small amount of propylene. In this case, the main role of Mo_2C is to initiate the dissociation of CH_3Cl to produce CH_3 surface species. As was mentioned above, Mo_2C is less reactive towards the complete decomposition of hydrocarbon fragments as compared to highly dispersed Pt metals, nevertheless, it also promotes their decomposition to surface carbon

$$CH_{3(a)} = CH_{2(a)} + H_{(a)} \quad (8)$$

$$CH_{2(a)} = C_{(a)} + H_{2(g)} \quad (9)$$

and the formation of methane. This latter reaction may occur in the hydrogenation of CH_x species or in the disproportionation of CH_3

$$4CH_{3(a)} = 3CH_{4(g)} + C_{(a)} \quad (10)$$

In addition, we may also count with the decomposition of ethylene on Mo_2C surface.

The situation was different on ZSM-5, which itself is an effective catalyst for the conversion of CH_3Cl into C_2–C_4 compounds [5–8]. The formation of these compounds are described by the Eqs. 4–6. We expected that due to the promoting effect of Mo_2C on the dissociation of CH_3Cl (Eq. 3), a new route is opened for the production of carbene, CH_2, which, reacting with methoxy species, yields ethylene. This expectation was, however, only partially fulfilled as the decomposition of CH_3Cl occurred at somewhat lower temperature on Mo_2C-doped ZSM-5 as compared to undoped ZSM-5. But at higher temperature, when ZSM-5 is active in the transformation of CH_3Cl into other compounds, the effect of Mo_2C could not come in prominence.

5. Conclusions

(i) CH_3Cl adsorbs reversibly on ZSM-5 at 300 K. Stronger interaction occurred at and above 473 K, when methoxy species and alkene carbocation were identified by IR spectroscopy. (ii) The catalytic decomposition of CH_3Cl proceeded with well measurable rate at and above 673 K yielding propylene, ethylene, butane, methane and benzene in decreasing selectivities. The formation of these products is described by the transient appearance of ethoxide and propoxide. (iii) Mo_2C only slightly influences the processes occurring on the active ZSM-5 catalyst. (iv) Its catalytic effect was exhibited in the case of Mo_2C/SiO_2 when it promoted the cleavage of C–Cl bond in the CH_3Cl.

Acknowledgements

This work was supported by the OTKA F025610.

Appendix

Numerical data, together with product analyses for each individual measurements plotted in Figs. 1 and 2 are compiled in Tables A1–A16 below.

Table A1
Dependence of the oxidation of tetralin with O_2 on the concentration of catalysts ALCl and ion-pair AL-V(V), respectively
pH: 9.00

log[ALCl]	log[AL-V(V)]	ΔO_2 (mmol)	ΔO_{act}^{corr} (mmol)	Δ[T-one] (mmol)	Δ[T-ol] (mmol)	Σ[products] − ΔO_2
−5.824	–	0.115	0.059	0.000	0.054	−0.002
−4.824	–	0.140	0.099	0.000	0.084	0.043
−3.824	–	0.161	0.138	0.000	0.046	0.023
−3.312	–	0.295	0.238	0.000	0.115	0.058
−2.824	–	0.633	0.536	0.000	0.190	0.093
−2.312	–	1.081	0.616	0.195	0.557	0.287
−1.824	–	1.642	0.736	0.347	1.129	0.570
−1.312	–	1.687	0.855	0.252	1.115	0.535
−0.824	–	1.528	1.133	0.298	0.186	0.089
−5.824	−5.824	0.037	0.019	0.000	0.018	0.000
−4.824	−4.824	0.084	0.059	0.000	0.050	0.025
−3.824	−3.824	0.408	0.298	0.031	0.135	0.056
−3.312	−3.312	0.883	0.516	0.090	0.553	0.276
−2.824	−2.824	1.309	0.357	0.778	0.376	0.202
−2.312	−2.312	2.005	0.059	1.507	0.899	0.460
−1.824	−1.824	0.748	0.099	0.654	0.034	0.038
−0.824	−0.824	0.113	−0.100	0.213	0.000	0.000

Conditions: 2.759 M tetralin + 0.0125 M *t*-BHP + the corresponding catalyst dissolved in 8.00 cm^3 chlorobenzene.

Table A2
Dependence of the oxidation of tetralin with O_2 on the concentration of catalysts ALCl and ion-pair AL-V(V), respectively
pH: 7.01

log[ALCl]	log[AL-V(V)]	ΔO_2 (mmol)	ΔO_{act}^{corr} (mmol)	Δ[T-one] (mmol)	Δ[T-ol] (mmol)	Σ[products] − ΔO_2
−5.824	–	0.178	0.178	0.000	0.055	0.055
−4.824	–	0.666	0.516	0.012	0.270	0.132
−3.824	–	1.573	1.054	0.465	0.128	0.074
−3.312	–	1.758	1.153	0.332	0.517	0.244
−2.824	–	1.808	1.134	0.364	0.617	0.307
−2.312	–	1.861	1.213	0.288	0.706	0.346
−1.824	–	1.935	1.332	0.224	0.733	0.354
−1.312	–	1.448	0.847	0.125	0.746	0.270
−0.824	–	1.078	0.716	0.186	0.284	0.108
−5.824	−5.824	0.068	0.059	0.000	0.009	0.000
−4.824	−4.824	0.348	0.206	0.097	0.120	0.075
−3.824	−3.824	1.200	0.437	0.475	0.582	0.289
−3.312	−3.312	1.668	0.537	0.933	0.423	0.225
−2.824	−2.824	2.125	0.457	1.040	1.206	0.578
−2.312	−2.312	0.310	−0.001	0.166	0.263	0.119
−1.824	−1.824	0.088	−0.028	0.000	0.117	0.001
−0.824	−0.824	0.123	−0.100	0.000	0.222	−0.001

Conditions: 2.759 M tetralin + 0.0125 M *t*-BHP + the corresponding catalyst dissolved in 8.00 cm^3 chlorobenzene.

Table A3
Dependence of the oxidation of tetralin with O_2 on the concentration of catalysts ALCl and ion-pair AL-V(V), respectively
pH: 6.38

log[ALCl]	log[AL-V(V)]	ΔO_2 (mmol)	ΔO_{act}^{corr} (mmol)	Δ[T-one] (mmol)	Δ[T-ol] (mmol)	Σ[products] − ΔO_2
−5.204	–	0.302	0.281	0.000	0.017	−0.004
−4.204	–	0.867	0.676	0.043	0.283	0.135
−3.903	–	0.950	0.636	0.112	0.344	0.138
−3.505	–	1.217	0.815	0.222	0.356	0.176
−3.204	–	1.540	1.412	0.149	0.001	0.022
−2.903	–	1.818	1.213	0.383	0.426	0.209
−2.505	–	2.175	1.451	0.326	0.739	0.341
−2.204	–	2.682	1.651	0.623	0.799	0.391
−1.903	–	2.035	1.293	0.553	0.351	0.162
−1.602	–	1.678	0.616	0.679	0.768	0.385
−5.204	−5.248	0.114	0.079	0.035	0.002	0.002
−4.509	−4.549	0.435	0.298	0.116	0.043	0.022
−4.204	−4.248	0.741	0.377	0.309	0.704	0.649
−3.903	−3.947	1.034	0.377	0.466	0.397	0.206
−3.505	−3.549	1.384	0.377	0.658	0.750	0.401
−2.903	−2.947	2.037	0.258	1.716	0.115	0.052
−2.505	−2.549	1.099	0.178	0.841	0.160	0.080
−2.204	−2.248	0.170	−0.028	0.274	0.000	0.076
−1.903	−1.947	0.098	−0.100	0.165	0.000	−0.033

Conditions: 2.759 M tetralin + 0.0125 M *t*-BHP + the corresponding catalyst dissolved in 8.00 cm^3 chlorobenzene.

Table A4
Dependence of the oxidation of tetralin with O_2 on the concentration of catalysts ALCl and ion-pair AL-V(V), respectively
pH: 4.50

log[ALCl]	log[AL-V(V)]	ΔO_2 (mmol)	ΔO_{act}^{corr} (mmol)	Δ[T-one] (mmol)	Δ[T-ol] (mmol)	Σ[products] − ΔO_2
−5.824	–	0.093	0.087	0.000	0.013	0.007
−4.824	–	0.494	0.461	0.000	0.067	0.034
−3.824	–	1.056	0.895	0.063	0.198	0.100
−3.312	–	1.449	0.915	0.184	0.676	0.326
−2.824	–	2.087	1.197	0.576	0.628	0.314
−2.312	–	2.649	1.169	0.903	1.192	0.615
−1.824	–	3.233	1.929	1.256	0.086	0.038
−1.312	–	2.671	1.248	0.693	1.452	0.722
−0.824	–	2.183	1.531	0.411	0.502	0.261
−5.824	−5.824	0.077	0.059	0.000	0.039	0.021
−4.824	−4.824	0.189	0.138	0.000	0.096	0.045
−3.824	−3.824	0.795	0.457	0.111	0.453	0.226
−3.312	−3.312	1.370	0.457	0.490	0.852	0.429
−2.824	−2.824	2.290	0.387	1.419	0.981	0.497
−2.312	−2.312	3.327	0.417	2.187	1.468	0.745
−1.824	−1.824	3.470	−0.100	3.566	0.000	−0.004
−1.312	−1.312	2.008	−0.100	2.108	0.000	0.000
−0.824	−0.824	0.887	−0.100	0.987	0.000	0.000

Conditions: 2.759 M tetralin + 0.0125 M *t*-BHP + the corresponding catalyst dissolved in 8.00 cm^3 chlorobenzene.

Table A5
Dependence of the oxidation of tetralin with O_2 on the concentration of catalysts ALCl and ion-pair AL-V(V), respectively
pH: 3.00

log[ALCl]	log[AL-V(V)]	ΔO_2 (mmol)	ΔO_{act}^{corr} (mmol)	Δ[T-one] (mmol)	Δ[T-ol] (mmol)	Σ[products] − ΔO_2 (mmol)
−5.824	–	0.111	0.099	0.000	0.024	0.012
−4.824	–	0.226	0.178	0.000	0.095	0.047
−3.824	–	0.732	0.616	0.000	0.229	0.113
−3.312	–	1.149	0.855	0.100	0.409	0.215
−2.824	–	1.568	1.193	0.268	0.202	0.095
−2.312	–	1.873	1.173	0.471	0.439	0.210
−1.824	–	2.098	1.551	0.459	0.173	0.085
−1.312	–	2.176	1.492	0.560	0.145	0.021
−0.824	–	2.069	1.153	0.742	0.349	0.175
−5.824	−5.824	0.100	0.091	0.000	0.0090	0.000
−4.824	−4.824	0.252	0.258	0.000	0.000	0.006
−3.824	−3.824	0.670	0.537	0.036	0.218	0.121
−2.824	−2.824	1.712	0.537	0.902	0.598	0.325
−2.312	−2.312	3.056	0.557	2.377	0.241	0.119
−1.824	−1.824	4.445	−0.100	3.960	1.139	0.554
−1.568	−1.568	3.948	−0.100	4.032	0.000	−0.016
−1.312	−1.312	3.651	−0.100	3.738	0.000	−0.013
−0.824	−0.824	1.760	−0.100	1.854	0.000	−0.006

Conditions: 2.759 M tetralin + 0.0125 M *t*-BHP + the corresponding catalysts dissolved in 8.00 cm^3 chlorobenzene.

Table A6
Dependence of the oxidation of tetralin with O_2 on the concentration of catalysts ALCl and ion-pair AL-V(V), respectively
pH: 4.50

log[ALCl]	log[AL-V(V)]	ΔO_2 (mmol)	ΔO_{act}^{corr} (mmol)	Δ[T-one] (mmol)	Δ[T-ol] (mmol)	Σ[products] − ΔO_2
−5.522	–	0.154	0.139	0.000	0.015	0.000
−5.000	–	0.295	0.258	0.000	0.076	0.039
−4.522	–	−0.689	0.497	0.199	0.002	0.009
−4.000	–	1.172	0.974	0.198	0.003	0.003
−3.522	–	1.283	0.935	0.371	0.007	0.030
−3.000	–	1.469	1.094	0.381	0.000	0.006
−2.522	–	1.619	0.895	0.407	0.682	0.365
−2.000	–	1.857	1.213	0.552	0.178	0.086
−1.520	–	1.520	1.332	0.201	0.004	0.017
−1.000	–	1.367	0.895	0.466	0.010	0.004
−6.000	−5.504	0.043	0.035	0.000	0.009	0.001
5.522	−5.027	0.069	0.051	0.000	0.018	0.000
−5.000	−4.504	0.141	0.099	0.034	0.006	−0.002
−4.522	−4.027	0.204	0.138	0.000	0.057	−0.009
−4.000	−3.504	0.368	0.258	0.113	0.000	0.003
−3.522	−3.027	0.859	0.317	0.429	0.224	0.111
−2.522	−2.027	2.426	0.258	1.437	1.505	0.774
−2.000	−1.504	3.168	0.059	2.527	1.190	0.608
−1.522	−1.027	3.808	−0.001	2.481	2.578	1.250
−1.240	−0.744	3.946	−0.068	2.945	2.091	1.022
−1.000	−0.504	3.725	−0.100	2.963	1.698	0.836

Conditions: 2.759 M tetralin + 0.0125 M *t*-BHP + the corresponding catalyst dissolved in 8.00 cm^3 chlorobenzene.

Table A7
Dependence of the oxidation of tetralin with O_2 on the concentration of catalysts ALCl and ion-pair AL-V(V), respectively
pH: 3.62

log[ALCl]	log[AL-V(V)]	ΔO_2 (mmol)	ΔO_{act}^{corr} (mmol)	Δ[T-one] (mmol)	Δ[T-ol] (mmol)	Σ[products] − ΔO_2
−5.522	–	0.329	0.298	0.027	0.003	−0.001
−5.000	–	0.519	0.417	0.036	0.077	0.011
−4.522	–	0.639	0.616	0.023	0.019	0.019
−4.000	–	0.811	0.696	0.065	0.061	0.011
−3.488	–	1.320	0.895	0.209	0.436	0.220
−3.000	–	1.945	1.332	0.586	0.053	0.026
−2.698	–	2.392	1.512	0.606	0.576	0.302
−2.000	–	1.642	1.253	0.386	0.000	−0.003
−1.488	–	1.379	0.656	0.630	0.197	0.104
−1.000	–	1.119	0.616	0.499	0.003	−0.001
−5.509	−4.995	0.103	0.103	0.000	0.007	0.007
−4.509	−3.995	0.279	0.274	0.067	0.000	0.062
−3.509	−2.995	0.768	0.470	0.334	0.000	0.036
−2.986	−2.472	1.405	0.429	0.980	0.040	0.105
−2.509	−1.995	2.238	0.449	1.684	0.057	−0.048
−2.204	−1.705	2.810	0.298	2.505	0.002	−0.005
−1.903	−1.404	3.288	0.218	3.068	0.002	0.000
−1.426	−0.927	4.011	−0.100	4.116	0.000	0.005
−1.225	−0.726	3.824	−0.100	3.885	0.000	−0.039
−0.924	−0.407	3.493	−0.100	3.600	0.000	0.007

Conditions: 2.759 M tetralin + 0.0125 M *t*-BHP + the corresponding catalyst dissolved in 8.00 cm^3 chlorobenzene.

Table A8
Dependence of the oxidation of tetralin with O_2 on the concentration of catalysts ALCl and ion-pair AL-V(V), respectively
pH: 3.00

log[ALCl]	log[AL-V(V)]	ΔO_2 (mmol)	ΔO_{act}^{corr} (mmol)	Δ[T-one] (mmol)	Δ[T-ol] (mmol)	Σ[products] − ΔO_2
−5.435	–	0.223	0.206	0.020	0.003	0.006
−4.912	–	0.310	0.206	0.008	0.076	−0.020
−4.435	–	0.466	0.410	0.050	0.005	−0.001
−3.912	–	0.789	0.756	0.042	0.000	0.009
−3.435	–	1.210	0.879	0.308	0.007	−0.016
−2.912	–	1.875	1.368	0.467	0.067	0.027
−2.690	–	1.950	1.572	0.349	0.011	−0.018
−2.312	–	1.859	1.286	0.580	0.008	0.015
−2.096	–	1.609	1.368	0.197	0.023	−0.021
−1.903	–	1.145	0.858	0.253	0.020	−0.014
−1.602	–	0.599	0.470	0.098	0.029	−0.002
−5.440	−4.923	0.112	0.144	0.000	0.000	0.032
−4.440	−3.923	0.291	0.286	0.027	0.008	0.030
−3.903	−3.403	0.426	0.258	0.163	0.000	−0.005
−3.440	−2.923	0.762	0.516	0.100	0.084	−0.062
−2.917	−2.400	0.942	0.510	0.221	0.445	0.234
−2.315	−1.798	1.842	0.449	1.376	0.033	0.016
−1.950	−1.440	2.449	0.532	1.980	0.000	0.013
−1.602	−1.102	3.253	0.178	2.116	1.732	0.767
−1.397	−0.898	3.590	0.079	2.510	1.939	0.938
−1.225	−0.730	3.812	−0.100	3.918	0.000	0.006
−0.924	−0.424	3.717	−0.100	3.822	0.000	0.005

Conditions: 2.759 M tetralin + 0.0125 M *t*-BHP + the corresponding catalyst dissolved in 8.00 cm^3 chlorobenzene.

Table A9
Dependence of the oxidation of cyclohexene with O_2 on the concentration of catalysts ALCl and ion-pair AL-V(V), respectively
pH: 9.00

log[ALCl]	log[AL-V(V)]	ΔO_2 (mmol)	ΔO_{act}^{corr} (mmol)	Δ[Ch-E] (mmol)	Δ[Ch-ol] (mmol)	Σ[products] − ΔO_2
−5.824	–	0.461	0.457	0.010	0.000	0.006
−4.824	–	0.901	0.895	0.044	0.000	0.038
−3.824	–	1.154	0.994	0.035	0.118	−0.007
−3.312	–	1.657	1.412	0.035	0.204	−0.006
−2.824	–	2.194	1.691	0.055	0.447	−0.001
−2.312	–	2.257	1.571	0.162	0.518	−0.006
−1.824	–	2.314	1.392	0.055	0.876	0.009
−1.312	–	2.235	1.571	0.059	0.589	−0.016
−0.824	–	2.172	1.133	0.038	1.002	0.001
−5.824	−5.824	0.360	0.337	0.019	0.020	0.016
−4.824	−4.824	0.562	0.516	0.061	0.030	0.045
−3.824	−3.824	1.017	0.417	0.171	0.458	0.029
−3.312	−3.312	1.097	0.147	0.315	0.612	−0.023
−2.824	−2.824	1.424	0.099	0.361	0.942	−0.022
−2.312	−2.312	2.317	0.059	0.416	1.810	−0.032
−1.824	−1.824	3.365	0.019	0.371	2.910	−0.065
−1.678	−1.678	3.566	−0.001	0.282	3.290	0.005
−1.569	−1.569	3.220	−0.020	0.231	3.005	−0.004
−1.312	−1.312	2.013	−0.060	0.383	1.675	−0.015
−0.824	−0.824	0.121	−0.100	0.010	0.216	0.005

Conditions: 2.468 M cyclohexene + 0.0125 M *t*-BHP + the corresponding catalysts dissolved in 8.00 cm^3 chlorobenzene.

Table A10
Dependence of the oxidation of cyclohexene with O_2 on the concentration of catalysts ALCl and ion-pair AL-V(V), respectively
pH: 7.01

log[ALCl]	log[AL-V(V)]	ΔO_2 (mmol)	ΔO_{act}^{corr} (mmol)	Δ[Ch-E] (mmol)	Δ[Ch-ol] (mmol)	Σ[products] − ΔO_2
−5.824	–	0.895	0.815	0.032	0.085	0.037
−4.824	–	1.756	1.492	0.065	0.215	0.016
−3.824	–	2.025	1.432	0.114	0.489	0.010
−3.312	–	2.304	1.452	0.102	0.767	0.017
−2.824	–	2.578	1.630	0.090	0.846	−0.012
−2.312	–	2.697	1.531	0.096	1.132	0.062
−1.824	–	2.614	1.690	0.080	0.817	−0.027
−0.824	–	2.142	1.332	0.056	0.800	0.046
−5.824	−5.824	1.261	1.094	0.242	0.000	0.075
−4.824	−4.824	1.400	0.895	0.274	0.221	−0.010
−3.824	−3.824	1.596	0.218	0.402	0.966	−0.010
−3.312	−3.312	1.838	0.059	0.404	1.358	−0.017
−2.824	−2.824	2.409	0.099	0.516	1.794	0.000
−2.568	−2.568	3.100	0.051	0.347	2.709	0.007
−2.312	−2.312	3.807	−0.021	0.238	3.636	0.046
−2.195	−2.195	3.356	−0.032	0.240	3.170	0.022
−2.064	−2.064	2.948	−0.061	0.238	2.741	0.001
−1.824	−1824	0.841	−0.020	0.133	0.726	−0.002
−1.312	−1.312	0.195	−0.100	0.014	0.283	0.002
−0.824	−0.824	0.131	−0.100	0.023	0.225	0.017

Conditions: 2.468 M cyclohexene + 0.0125 M *t*-BHP + the corresponding catalysts dissolved in 8.00 cm^3 chlorobenzene.

Table A11
Dependence of the oxidation of cyclohexene with O_2 on the concentration of catalysts ALCl and ion-pair AL-V(V), respectively
pH: 6.38

log[ALCl]	log[AL-V(V)]	ΔO_2 (mmol)	ΔO_{act}^{corr} (mmol)	Δ[Ch-E] (mmol)	Δ[Ch-ol] (mmol)	Σ[products] − ΔO_2
−5.505	–	0.599	0.556	0.022	0.029	0.008
−5.204	–	0.935	0.934	0.043	0.000	0.042
−4.509	–	1.774	1.691	0.067	0.046	0.030
−4.204	–	2.257	1.850	0.095	0.328	0.016
−3.903	–	2.533	1.929	0.121	0.485	0.002
−3.204	–	2.814	1.770	0.254	0.783	−0.007
−2.903	–	2.847	1.909	0.114	0.810	−0.014
−2.204	–	3.002	1.810	0.102	1.080	−0.010
−1.903	–	3.035	1.730	0.176	1.123	−0.006
−1.602	–	2.712	1.531	0.108	1.053	−0.020
−0.999	–	2.059	1.531	0.099	0.428	−0.001
−5.505	−5.549	0.677	0.668	0.052	0.000	0.043
−4.509	−4.549	0.953	0.537	0.238	0.156	−0.022
−4.204	−4.248	0.969	0.198	0.319	0.435	−0.017
−3.903	−3.947	1.051	0.138	0.300	0.608	−0.005
−3.505	−3.549	1.482	0.059	0.507	0.811	−0.105
−3.204	−3.248	1.827	0.051	0.362	1.407	−0.007
−2.903	−2.947	2.444	0.039	0.470	1.927	−0.008
−2.505	−2.549	3.400	0.011	0.271	3.128	0.010
−2.204	−2.248	2.816	−0.068	0.157	2.720	−0.007
−2.028	−2.072	2.373	−0.076	0.245	2.190	−0.014
−1.903	−1.947	0.489	−0.068	0.042	0.544	0.029

Conditions: 2.468 M cyclohexene + 0.0125 M *t*-BHP + the corresponding catalyst dissolved 8.00 cm^3 chlorobenzene.

Table A12
Dependence of the oxidation of cyclohexene with O_2 on the concentration of catalysts ALCl and ion-pair AL-V(V), respectively
pH: 4.50

log[ALCl]	log[AL-V(V)]	ΔO_2 (mmol)	ΔO_{act}^{corr} (mmol)	Δ[Ch-E] (mmol)	Δ[Ch-ol] (mmol)	Σ[products] − ΔO_2
−5.824	–	0.839	0.815	0.005	0.013	−0.006
−4.824	–	1.402	1.372	0.047	0.000	0.017
−3.824	–	1.770	1.472	0.024	0.205	−0.069
−3.312	–	2.079	2.048	0.064	0.000	0.033
−2.824	–	2.409	1.466	0.032	0.912	0.001
−2.312	–	2.461	1.730	0.085	0.640	−0.006
−1.824	–	2.675	1.466	0.034	1.116	−0.059
−1.312	–	2.624	1.691	0.066	0.848	−0.019
−0.824	–	2.511	1.691	0.030	0.779	−0.011
−5.824	−5.824	0.623	0.616	0.024	0.000	0.017
−5.312	−5.312	0.880	0.815	0.042	0.027	0.004
−4.824	−4.824	1.094	0.895	0.067	0.127	−0.005
−4.312	−4.312	1.203	0.815	0.122	0.268	0.002
−3.824	−3.824	1.223	0.338	0.325	0.552	−0.008
−3.312	−3.312	1.705	0.118	0.520	1.052	−0.015
−2.824	−2.824	2.755	0.059	0.446	2.151	−0.099
−2.312	−2.312	3.908	−0.061	0.397	3.581	0.009
−1.824	−1.824	4.760	−0.100	0.214	4.641	−0.005
−1.312	−1.312	3.240	−0.100	0.071	3.267	−0.002
−0.824	−0.824	1.864	−0.100	0.045	1.918	−0.001

Conditions: 2.468 M cyclohexene + 0.0125 M *t*-BHP + the corresponding catalysts dissolved in 8.00 cm^3 chlorobenzene.

Table A13
Dependence of the oxidation of cyclohexene with O_2 on the concentration of catalysts ALCl and ion-pair AL-V(V), respectively
pH: 3.00

log[ALCl]	log[AL-V(V)]	ΔO_2 (mmol)	ΔO_{act}^{corr} (mmol)	Δ[Ch-E] (mmol)	Δ[Ch-ol] (mmol)	Σ[products] − ΔO_2
−5.824	–	1.086	0.994	0.015	0.091	0.014
−5.312		1.717	1.472	0.005	0.224	−0.016
−4.824	–	2.303	1.491	0.059	0.779	0.016
−3.824	–	2.522	1.507	0.060	0.940	−0.15
−3.312	–	2.739	2.248	0.072	0.422	0.003
−2.824	–	3.081	1.969	0.134	0.985	0.007
−2.312	–	2.948	2.566	0.046	0.327	−0.009
−1.824	–	2.880	1.663	0.068	1.157	0.008
−1.312	–	2.833	1.790	0.039	1.005	0.001
−0.824	–	2.767	1.468	0.050	1.248	−0.001
−5.824	−5.824	0.968	0.755	0.044	0.190	0.021
−5.312	−5.312	1.379	0.994	0.234	0.150	−0.001
−4.824	−4.824	1.834	1.094	0.189	0.543	−0.008
−3.824	−3.824	2.032	0.576	0.399	1.061	0.004
−3.312	−3.312	2.259	0.218	0.514	1.513	−0.014
−2.824	−2.824	2.935	0.039	0.351	2.514	−0.031
−2.569	−2.569	3.956	−0.040	0.546	3.400	−0.050
−2.312	−2.312	4.937	−0.060	0.605	4.359	−0.033
−2.064	−2.064	5.240	−0.060	0.421	4.863	−0.016
−1.824	−1.824	4.890	−0.080	0.231	4.672	−0.067
−1.312	−1.312	3.623	−0.100	0.149	3.542	−0.032
−0.824	−0.824	2.605	−0.100	0.071	2.599	−0.035

Conditions: 2.468 M cyclohexene + 0.0125 M *t*-BHP + the corresponding catalysts dissolved in 8.00 cm^3 chlorobenzene.

Table A14
Dependence of the oxidation of cyclohexene with O_2 on the concentration of catalysts ALCl and ion-pair AL-V(V), respectively
pH: 4.50

log[ALCl]	log[AL-V(V)]	ΔO_2 (mmol)	ΔO_{act}^{corr} (mmol)	Δ[Ch-E] (mmol)	Δ[Ch-ol] (mmol)	Σ[products] − ΔO_2
−6.000	–	0.567	0.454	0.015	0.099	−0.005
−5.522	–	0.989	0.974	0.017	0.000	0.002
−5.000	–	1.480	1.352	0.023	0.111	0.006
−4.522		1.746	1.332	0.029	0.380	−0.005
−4.000	–	1.969	1.531	0.069	0.357	−0.012
−3.522	–	2.109	1.492	0.050	0.600	0.033
−3.000	–	2.330	1.452	0.068	0.782	−0.028
−2.522	–	2.498	1.452	0.067	0.930	−0.049
−2.000	–	2.616	1.490	0.069	1.055	−0.002
−1.522	–	2.725	1.531	0.072	1.102	−0.020
−1.000	–	2.583	1.293	0.063	1.231	0.004
−6.000	−5.504	0.546	0.496	0.054	0.000	0.004
−5.000	−4.504	0.580	0.377	0.096	0.111	0.004
−4.522	−4.026	0.705	0.179	0.243	0.78	−0.005
−4.000	−3.504	0.849	0.417	0.255	0.192	0.015
−3.522	−3.027	1.266	0.059	0.391	0.773	−0.043
−3.000	−2.504	2.277	−0.029	0.582	1.689	−0.035
2.522	−2.027	3.724	−0.084	0.738	3.051	−0.019
−2.000	−1.504	5.091	−0.100	0.499	4.666	−0.026
−1.522	−1.027	4.203	−0.100	0.216	4.016	−0.071
−1.000	−0.504	3.214	−0.100	0.130	3.156	−0.028

Conditions: 2.468 M cyclohexene + 0.0125 M *t*-BHP + the corresponding catalysts dissolved in 8.00 cm^3 chlorobenzene.

Table A15
Dependence of the oxidation of cyclohexene with O_2 on the concentration of catalysts ALCl and ion-pair AL-V(V), respectively
pH: 3.62

log[ALCl]	log[AL-V(V)]	ΔO_2 (mmol)	ΔO_{act}^{corr} (mmol)	Δ[Ch-E] (mmol)	Δ[Ch-ol] (mmol)	Σ[products] − ΔO_2
−6.000	–	0.500	0.497	0.020	0.000	0.017
−5.698	–	0.682	0.676	0.030	0.000	0.024
−5.301	–	1.088	1.011	0.045	0.033	0.001
−5.000	–	1.397	1.332	0.049	0.015	−0.001
−4.602	–	1.742	1.492	0.066	0.172	−0.012
−4.124	–	1.800	1.492	0.059	0.234	−0.015
−3.602	–	1.856	1.452	0.083	0.330	0.009
−2.999	–	2.060	1.551	0.061	0.443	−0.005
−2.602	–	2.218	1.691	0.070	0.467	0.010
−2.301	–	2.388	1.810	0.098	0.476	−0.004
−1.903	–	2.550	1.890	0.086	0.564	−0.010
−1.602	–	2.674	1.850	0.070	0.746	−0.008
−1.301	–	1.620	1.173	0.027	0.430	0.010
−1.125	–	1.110	1.014	0.022	0.055	−0.019
−0.999	–	0.907	0.795	0.017	0.107	0.012
−5.810	−5.296	0.598	0.388	0.077	0.113	−0.020
−5.644	−5.130	0.575	0.437	0.066	0.0620	−0.010
−5.509	−4.995	0.570	0.347	0.081	0.150	0.008
−4.986	−4.472	0.285	0.164	0.083	0.036	−0.002
−4.509	−3.995	0.465	0.185	0.094	0.207	0.021
−3.945	−3.431	0.754	0.042	0.357	0.506	0.151
−3.509	−2.995	1.057	−0.019	0.249	0.820	−0.007
−2.986	−2.473	2.021	0.022	0.377	1.667	0.045
−2.685	−2.172	2.913	−0.019	0.349	2.560	−0.023
−2.301	−1.802	4.039	−0.068	0.318	3.784	−0.005
−1.903	−1.404	4.557	−0.100	0.304	4.338	−0.015
−1.602	−1.103	4.812	−0.100	0.301	4.564	0.047
−1.301	−0.802	3.880	−0.100	0.152	3.784	−0.044
−1.145	−0.647	3.517	−0.100	0.155	3.446	−0.016

Conditions: 2.468 M cyclohexene + 0.0125 M *t*-BHP + the corresponding catalysts dissolved in 8.00 cm^3 chlorobenzene.

Table A16
Dependence of the oxidation of cyclohexene with O_2 on the concentration of catalysts ALCl and ion-pair AL-V(V), respectively
pH: 3.00

log[ALCl]	log[AL-V(V)]	ΔO_2 (mmol)	ΔO_{act}^{corr} (mmol)	Δ[Ch-E] (mmol)	Δ[Ch-ol] (mmol)	Σ[products] − ΔO_2
−5.912	–	0.513	0.511	0.017	0.000	0.015
−5.435	–	0.782	0.695	0.033	0.058	0.004
−4.913	–	0.989	0.980	0.026	0.000	0.017
−4.435	–	1.129	1.009	0.031	0.111	0.022
−4.009	–	1.508	1.327	0.031	0.102	−0.048
−3.435	–	1.883	1.613	0.053	0.224	0.007
−2.912	–	2.399	1.816	0.090	0.501	0.008
−2.602	–	2.619	1.770	0.089	0.766	0.006
−2.213	–	2.777	1.939	0.134	0.732	0.028
−1.999	–	2.638	1.878	0.085	0.662	−0.013
−1.602	–	2.404	1.770	0.065	0.567	−0.002
−1.301	–	2.286	1.810	0.076	0.390	−0.010
−1.125	–	2.243	1.690	0.064	0.478	−0.011
−1.000	–	2.198	1.472	0.061	0.655	−0.010
−5.912	−5.399	0.414	0.316	0.061	0.023	−0.014
−5.435	−4.923	0.506	0.287	0.079	0.129	−0.011
−4.435	−3.923	0.571	0.075	0.088	0.380	−0.028
−3.435	−2.923	0.759	−0.018	0.195	0.561	−0.021
−2.912	−2.399	1.364	0.002	0.291	1.045	−0.026
−2.612	−2.098	2.152	−0.003	0.316	1.713	−0.126
−2.310	−1.798	2.964	−0.051	0.506	2.506	−0.003
−2.033	−1.521	3.809	−0.072	0.436	3.405	−0.040
−1.732	−1.220	4.836	−0.060	0.342	4.512	−0.042
−1.404	−1.059	3.643	−0.100	0.256	3.446	−0.041
−1.301	−0.806	3.396	−0.100	0.131	3.318	−0.047
−1.146	−0.651	2.920	−0.100	0.130	2.921	0.031

Conditions: 2.468 M cyclohexene + 0.0125 M *t*-BHP + the corresponding catalysts dissolved in 8.00 cm^3 chlorobenzene.

References

[1] W.J.M. Pieters, W.C. Conner, E.J. Carlson, Appl. Catal. 11 (1984) 35.
[2] G.A. Olah, Á. Molnár, in: G.A. Olah, Á. Molnár (Eds.), Hydrocarbon Chemistry, Wiley-Interscience, New York, 1995.
[3] K.J. Jeans, S. Halvorsen, E.B. Ofsted, in: D.M. Bibby, C.D. Chang, R.F. Howe, S. Yurchak (Eds.), Methane Conversion, Elsevier, Amsterdam, 1988, p. 491.
[4] P. Lersch, F. Bandermann, Appl. Catal. 75 (1991) 133.
[5] C.E. Taylor, R.P. Noceti, R.R. Schehl, in: D.M. Bibby, C.D. Chang, R.F. Howe, S. Yurchak (Eds.), Methane Conversion, Elsevier, Amsterdam, 1988, p. 483.
[6] C.D. Chang, Catal. Rev. — Sci. Eng. 25 (1983) 1.
[7] V.N. Rommanikov, K.G. Ione, Kinet. Katal. 25 (1984) 92.
[8] Y. Sun, S.M. Campbell, J.H. Lunsford, G.E. Lewis, D. Palke, L.-M. Tau, J. Catal. 143 (1993) 32.
[9] D. Wang, J.H. Lunsford, M.P. Rosynek, Top. Catal. 3 (4) (1996) 299.
[10] F. Solymosi, A. Szõke, Catal. Lett. 39 (1996) 157.
[11] F. Solymosi, J. Cserényi, A. Szõke, T. Bánsági, A. Oszkó, J. Catal. 165 (1997) 150.
[12] D. Wang, J.H. Lunsford, M.P. Rosynek, J. Catal. 169 (1997) 347.
[13] L. Wang, L. Tao, M. Xie, G. Xu, Catal. Lett. 21 (1993) 35.
[14] Y. Xu, S. Liu, L. Wang, M. Xie, X. Guo, Catal. Lett. 30 (1995) 135.
[15] F. Solymosi, A. Erdõhelyi, A. Szõke, Catal. Lett. 32 (1995) 43.
[16] A. Szõke, F. Solymosi, Appl. Catal. A 142 (1996) 361.
[17] F. Solymosi, R. Németh, L. Óvári, L. Egri, to be published.
[18] J.S. Lee, S.T. Oyama, M. Boudart, J. Catal. 106 (1987) 125.
[19] F. Solymosi, L. Bugyi, A. Oszkó, I. Horváth, J. Catal. 185 (1999) 249.
[20] F. Solymosi, L. Bugyi, A. Oszkó, Catal. Lett. 57 (1999) 103.
[21] F. Solymosi, in: E.G. Derouane (Ed.), Catalytic Activation and Functionalisation of Light Alkanes, Kluwer Academic Publishing, Netherlands, 1998, pp. 369–388.
[22] D.C Harris, M.D. Bertolucci, Symmetry and Spectroscopy, Oxford Univ. Press, New York, 1978, p. 224.
[23] B. Frühberger, I.G. Chen, J. Am. Chem. Soc. 118 (1996) 11599.

[24] M.A. Chesters, C. De La Cruz, P. Gardner, E.M. McCash, P. Pudney, G. Shahid, N. Sheppard, J. Chem. Soc., Faraday Trans. 86 (15) (1990) 2757.
[25] Y. Suda, T. Morimoto, M. Nagao, Langmuir 3 (1987) 99.
[26] M.D. Driessen, V.H. Grassian, Langmuir 14 (1998) 1411.
[27] E.A. Wovchko, J.C. Camp, J.A. Glass Jr., J.T. Yates Jr., Langmuir 11 (1995) 2592.
[28] Z. Kónya, I. Hannus, I. Kiricsi, Appl. Catal. B 8 (1996) 391.
[29] J.E. Crowell, T.P. Beebe Jr., J.T. Yates Jr., J. Chem. Phys. 87 (1987) 3668.
[30] T.P. Beebe Jr., J.E. Crowell, J.T. Yates Jr., J. Phys. Chem. 92 (1988) 1296.
[31] J. Raskó, I. Bontovics, F. Solymosi, J. Catal. 143 (1993) 138.
[32] J. Raskó, F. Solymosi, Catal. Lett. 46 (1997) 153.
[33] J. Raskó, F. Solymosi, Catal. Lett. 54 (1998) 49.
[34] I. Kiricsi, H. Förster, Gy. Tasi and, J.B. Nagy, Chem. Rev. 99 (1999) 2085.